A TURBULENT BOUNDARY LAYER WITH INJECTION INTO A COMPRESSIBLE FLUID WITH A PRESSURE GRADIENT

N. S. Krest'yaninova

UDC 532.517.4

We use the semiempirical theory of turbulence to study the effect exerted by the input of a homogeneous material through the main flow on the friction and on the heat transfer in the turbulent boundary layer, in a compressible fluid with a pressure gradient.

In the case of a perfect gas, the equations describing the motion of the fluid in a flat-profile boundary layer have the form [1]

$$\frac{\partial}{\partial x}(\rho v_x)+\frac{\partial}{\partial y}(\rho v_y)=0, \tag{1}$$

$$\rho v_x\frac{\partial v_x}{\partial x}+\rho v_y\frac{\partial v_x}{\partial y}=-\frac{\partial p}{\partial x}+\frac{\partial \tau}{\partial y}, \tag{2}$$

$$\frac{\partial p}{\partial y}=0, \tag{3}$$

$$\rho v_x\frac{\partial h}{\partial x}+\rho v_y\frac{\partial h}{\partial y}=v_x\frac{\partial p}{\partial x}+\frac{\partial q}{\partial y}+\tau\frac{\partial v_x}{\partial y}, \tag{4}$$

$$\frac{\rho}{\rho_\delta}=\frac{h_\delta}{h} \tag{5}$$

with the boundary conditions

$$\begin{gathered}\text{when } y=0\quad v_x=0,\quad v_y=v_\omega,\quad h=h_\omega\quad\text{or}\quad q=q_\omega,\\ \text{when } y=\delta\quad v_x=u_\delta,\quad h=h_\delta.\end{gathered} \tag{6}$$

In the laminar sublayer ($y \le \delta_l$), as is well known,

$$\tau=\mu\frac{\partial v_x}{\partial y}, \tag{7}$$

$$q=\frac{\lambda}{c_p}\frac{\partial h}{\partial y}. \tag{8}$$

Further, it is assumed that μ is proportional to h. The surface friction and the heat flow, according to the semiempirical theory, are determined for the case in which $y \ge \delta_l$ by the equations

$$\tau=\rho l^2\left(\frac{\partial v_x}{\partial y}\right)^2, \tag{9}$$

$$q=\rho l l_t\frac{\partial v_x}{\partial y}\frac{\partial h}{\partial y}. \tag{10}$$

Subsequently we will assume that $l = ky$ and $l_t = \tilde{k}y$. The numbers k and $\tilde{k}$ are associated by the relationship $Pr_t = k/\tilde{k}$ (see [2], p. 283). We will present the heat content in the form of a function of the longitudinal velocity component. For this we turn to the Crocco variables $x \to x_1$ and $y \to v_x(x, y)$. The energy equation

Zhdanov State University, Leningrad. Translated from Inzhenerno-Fizicheskii Zhurnal, Vol. 16, No. 6, pp. 989-1001, June, 1969. Original article submitted July 29, 1968.

in these variables is written in the form

$$\rho v_x \frac{\partial h}{\partial x_1} + \frac{\partial h}{\partial v_x}\left(-\frac{\partial p}{\partial x_1} + \frac{\partial \tau}{\partial y}\right) = v_x \frac{\partial p}{\partial x_1} + \frac{\partial q}{\partial y} + \tau \frac{\partial v_x}{\partial y}.$$

Recalling the estimate from [3], we neglect the first term of the last equation. It is then written as follows:

$$\frac{\partial}{\partial v_x}\left[\frac{1}{\mathrm{Pr}}\frac{\partial h}{\partial v_x}\right]\tau + \frac{1}{\mathrm{Pr}}\frac{\partial h}{\partial v_x}\left[(1-\mathrm{Pr})\frac{\partial \tau}{\partial v_x} + \mathrm{Pr}\frac{\frac{\partial p}{\partial x}}{\frac{\partial v_x}{\partial y}}\right] + \tau + v_x \frac{\frac{\partial p}{\partial x}}{\frac{\partial v_x}{\partial y}} = 0. \tag{11}$$

We solve the thermal problem by the method of successive approximations. In the zeroth approximation we neglect the terms containing $\partial p/\partial x$ in (11), i.e., we assume that the same form of the function between the heat content and the velocity is retained in flows with gradients as in the streamlining of a plate. Then, following ([2], p. 287), we can write

$$h_0 = h_{\omega 0} + \left(\frac{\partial h}{\partial \varphi}\right)_{\omega 0} S_0(\varphi) - u_\delta^2 R_0(\varphi),$$

$$S_0(\varphi) = \frac{1}{\mathrm{Pr}_\omega}\int_0^\varphi \mathrm{Pr}\exp\left[-\int_0^\varphi (1-\mathrm{Pr})\, d\ln\frac{\tau}{\tau_\omega}\right] d\varphi, \tag{12}$$

$$R_0(\varphi) = \int_0^\varphi \mathrm{Pr}\exp\left[-\int_0^\varphi (1-\mathrm{Pr})\, d\ln\frac{\tau}{\tau_\omega}\right]\left\{\int_0^\varphi \exp\left[\int_0^\varphi (1-\mathrm{Pr})\, d\ln\frac{\tau}{\tau_\omega}\right] d\varphi\right\} d\varphi,$$

$$\left(\frac{\partial h}{\partial \varphi}\right)_{\omega 0} = \frac{h_\delta + u_\delta^2 R_0(1) - h_{\omega 0}}{S_0(1)}. \tag{13}$$

To find $S_0(\varphi)$ and $R_0(\varphi)$ we have to know the distribution of the frictional shearing stresses across the boundary layer. As earlier in [1], we assume

$$\tau = \tau_\omega (1 + P\varphi),$$

where

$$P = \frac{\rho_\omega v_\omega u_\delta}{\tau_\omega} + \frac{\mu_\omega u_\delta}{\tau_\omega^2}\frac{\partial p}{\partial x}. \tag{14}$$

We introduce the notation

$$b = \frac{\rho_\omega v_\omega}{\rho_\delta u_\delta}, \quad A = \frac{b}{\frac{c_f}{2}}, \quad B = \frac{\frac{\partial p}{\partial x}\mu_\delta}{\rho_\delta^2 u_\delta^3}.$$

Then

$$P = A + \frac{B\tilde{h}_\omega}{\left(\frac{c_f}{2}\right)^2}.$$

Assuming $\mathrm{Pr}_t = 1$, and if we assume that Pr_l is constant across the boundary layer, after integration we obtain the following expressions for $S_0(\varphi)$ and $R_0(\varphi)$:

when $y \leq \delta_l$

$$S_{l0}(\varphi) = \frac{(1+P\varphi)^{\mathrm{Pr}} - 1}{P\,\mathrm{Pr}},$$

$$R_{l0}(\varphi) = \frac{\mathrm{Pr}}{P^2(2-\mathrm{Pr})}\left[\frac{(1+P\varphi)^2}{2} + \frac{2-\mathrm{Pr}}{2\mathrm{Pr}} - \frac{(1+P\varphi)^{\mathrm{Pr}}}{\mathrm{Pr}}\right],$$

when $y \geq \delta_l$

$$S_0(\varphi) = S_{l0}(\varphi_l) + \frac{\tilde{\tau}_л^{\mathrm{Pr}-1}}{\mathrm{Pr}}(\varphi - \varphi_л),$$

$$R_0(\varphi) = R_{l0}(\varphi_l) + (\tilde{\tau}_l - \tilde{\tau}_l^{\mathrm{Pr}-1}) \frac{\varphi - \varphi_l}{P(2-\mathrm{Pr})} + \frac{(\varphi - \varphi_l)^2}{2}.$$

Initially integrating (7), and then (9) in conjunction with (5), (12), and (14), we find the velocity profiles in the following form:

in the laminar sublayer

$$y = \frac{\mu_\delta}{\rho_\delta u_\delta \frac{c_f}{2}} \left[\frac{\ln \tilde{\tau}_l}{P} \tilde{h}_{\omega 0} + \frac{1}{P^2} \left(\frac{\partial \tilde{h}}{\partial \varphi} \right)_{\omega 0} \left(\frac{\tilde{\tau}_l^{\mathrm{Pr}} - 1}{\mathrm{Pr}^2} - \frac{\ln \tilde{\tau}_l}{\mathrm{Pr}} \right) + \frac{\tilde{u}_\delta^2}{P^3} \left(\frac{\tilde{\tau}_l^{\mathrm{Pr}} - 1}{\mathrm{Pr}(2-\mathrm{Pr})} - \frac{\mathrm{Pr}(\tilde{\tau}_l^2 - 1)}{4(2-\mathrm{Pr})} - \frac{\ln \tilde{\tau}_l}{2} \right) \right], \tag{15}$$

in the turbulent portion of the flow

$$y = \delta_l \exp\left[\frac{k}{\sqrt{\frac{c_f}{2}}} \int\limits_{\varphi_l}^{\varphi} \frac{d\varphi}{\sqrt{\tilde{\tau} \tilde{h}}} \right]. \tag{16}$$

From the condition

$$\left(\frac{\partial \varphi}{\partial y} \right)_{y=\delta_l - 0} = k_1 \left(\frac{\partial \varphi}{\partial y} \right)_{y=\delta_l + 0}$$

we find

$$\delta_l = \frac{k_1 \mu_\delta (\tilde{h}_l)^{3/2}}{k \rho_\delta u_\delta \sqrt{\frac{c_f}{2} \tilde{\tau}_l}}. \tag{17}$$

The two equations (15) and (17) allow us to find the relationship between δ_l and $c_f/2$ and between φ_l and $c_f/2$. Assuming $y = \delta$, as well as $\varphi = 1$, and considering (17), from (16) we find the relationship which associates δ with $c_f/2$. The second equation for δ and $c_f/2$ is found from the solution of the integral Karman relation

$$\frac{d\delta^{**}}{dx} + \frac{1}{u_\delta} \frac{du_\delta}{dx} (2\delta^{**} + \delta^*) = \frac{c_f}{2} + b. \tag{18}$$

We present the quantities δ^* and δ^{**} in the form

$$\delta^* = \delta - \frac{\mu_\delta}{\rho_\delta u_\delta \frac{c_f}{2}} \left[\frac{\varphi_g}{P} - \frac{\ln \tilde{\tau}_g}{P^2} \right] - \frac{k}{\sqrt{\frac{c_f}{2}}} \int\limits_{\varphi_l}^{1} \frac{y \varphi d\varphi}{\tilde{h} \sqrt{\tilde{h} \tilde{\tau}}},$$

$$\delta^{**} = \frac{\mu_\delta}{\rho_\delta u_\delta \frac{c_f}{2}} \left[\frac{\varphi_g}{P} - \frac{\ln \tilde{\tau}_g}{P^2} + \frac{1}{P^3} \left(2\tilde{\tau}_g - \frac{\tilde{\tau}_g^2}{2} - \ln \tilde{\tau}_л - \frac{3}{2} \right) \right] - \frac{k}{\sqrt{\frac{c_f}{2}}} \int\limits_{\varphi_g}^{1} \frac{(\varphi - \varphi)^2 y \, d\varphi}{\tilde{h} \sqrt{\tilde{h} \tilde{\tau}}}.$$

Because of the complexity of (18), as well as because of the impossibility of analytically taking the integrals in the expressions for δ^* and δ^{**}, the problem was solved numerically.

Leaving the discussion of the results from the numerical calculation for later, let us return to the solution of the energy equation in the next (the first) approximation, giving consideration to terms with $\partial p / \partial x$. We write the solution of (11) in the form

$$\tilde{h}_1 = \tilde{h}_{\omega 1} + \left(\frac{\partial \tilde{h}}{\partial \varphi} \right)_{\omega 1} S_1(\varphi) - \tilde{u}_\delta^2 R_1(\varphi),$$

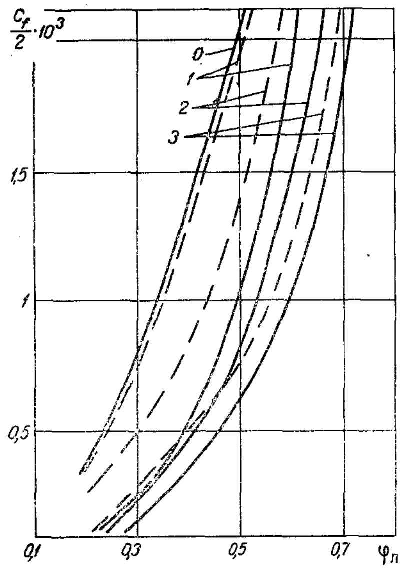

Fig. 1. Variation in the coefficient of surface friction as a function of the velocity at the edge of the laminar sublayer for various values of α, c, and M_{in}: 0) M_{in} = 0; 1) 0.8; 2) 3.0; 3) 5.0; the solid curves are for h_ω with a value of 5, and the dashed curves are for a value of 1.

where

$$S_1(\varphi) = \frac{1}{\mathrm{Pr}_\omega}\int_0^\varphi \mathrm{Pr}\exp\left[-\int_0^\varphi (1-\mathrm{Pr})\,d\ln\tilde{\tau} - \int_0^\varphi \mathrm{Pr}\frac{\frac{\partial p}{\partial x}}{\tau\frac{\partial\varphi}{\partial y}}d\varphi\right]d\varphi;$$

$$R_1(\varphi) = \int_0^\varphi \mathrm{Pr}\exp\left[-\int_0^\varphi (1-\mathrm{Pr})\,d\ln\tilde{\tau} - \int_0^\varphi \mathrm{Pr}\frac{\frac{\partial p}{\partial x}}{\tau\frac{\partial\varphi}{\partial y}}d\varphi\right]$$

$$\times\left\{\int_0^\varphi\left[1+\frac{\varphi\frac{\partial p}{\partial x}}{\tau\frac{\partial\varphi}{\partial y}}\right]\exp\left[\int_0^\varphi (1-\mathrm{Pr})\,d\ln\tilde{\tau} + \int_0^\varphi \mathrm{Pr}\frac{\frac{\partial p}{\partial x}}{\tau\frac{\partial\varphi}{\partial y}}d\varphi\right]d\varphi\right\}d\varphi.$$

Since Pr_l and Pr_t, as well as the relationship between $\partial\varphi/\partial y$ and φ are different in the laminar sublayer and in the turbulent portion of the flow, in connection with the adopted two-layer scheme we will find the form of the functions relating h to φ separately for the different layers. To find $S_1(\varphi)$ and $R_1(\varphi)$, in addition to $\tau(\varphi)$, we also have to know $\partial\varphi(\varphi)/\partial y$. This quantity will be found from (7) and (9), provided we take the relationship between h and φ from the zeroth approximation. Let us present $S_1(\varphi)$ and $R_1(\varphi)$ in the form of Taylor series in the vicinity of φ = 0 in the region of the laminar sublayer and in the vicinity of $\varphi = \varphi_l$ in the turbulent portion of the flow. Thus,

when $y \leq \delta_l$

$$S_l(\varphi) = \sum_{n=0}^{\infty} S_l^{(n)}(0)\frac{\varphi^n}{n!},\qquad R_l(\varphi) = \sum_{n=0}^{\infty} R_l^{(n)}(0)\frac{\varphi^n}{n!}, \tag{19}$$

when $y \geq \delta_l$

$$S_t(\varphi) = \sum_{n=0}^{\infty} S_t^{(n)}(\varphi_l)\frac{(\varphi-\varphi_h)^n}{n!},\qquad R_t(\varphi) = \sum_{n=0}^{\infty} R_t^{(n)}(\varphi_l)\frac{(\varphi-\varphi_h)^n}{n!}. \tag{20}$$

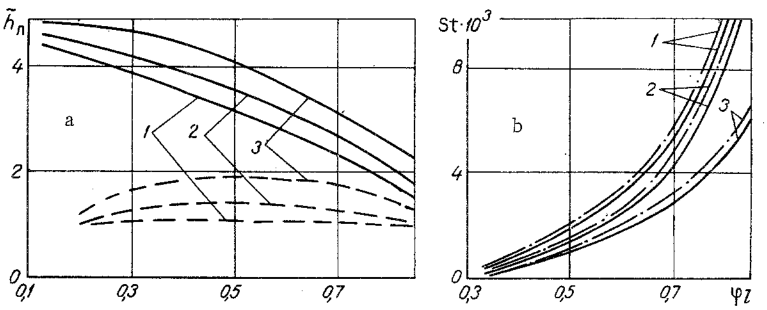

Fig. 2. Variation in heat content as a function of the velocity at the edge of the laminar sublayer (a) and the change in St as a function of φ_l for various values of c (b). The solid curves denote c = 0, the dash–dot curves denote 0.01. The notation is the same as in Fig. 1.

the coefficients of the series are written as follows:

when $y \leq \delta_l$

$$S_{l1}(0) = 0, \quad S'_{l1}(0) = 1,$$

$$S_l^{(n)}(0) = \sum_{m=0}^{n-2} \frac{(n-2)!\, S_{l1}^{(n-m-1)}(0)}{(n-m-2)!} \left[(-1)^{m+1} (1 - \mathrm{Pr}_l) \frac{p^{m+1}}{\tilde{\tau}^{m+1}} + \mathrm{Pr}_l \frac{\frac{\partial p}{\partial x}}{\tau_\omega} \sum_{k=0}^{m} (-1)^{k+1} \frac{p^k}{(m-k)!\, \tilde{\tau}^{k+1}} \left(\frac{\partial^{m+1-k} y}{\partial \varphi^{m+1-k}} \right)_{\omega 0} \right], \tag{21}$$

$$n = 2, 3, \ldots,$$

$$R_l(0) = 0, \quad R'_l(0) = 0,$$

$$R_{l1}^{(n)}(0) = \mathrm{Pr}_l \sum_{m=0}^{n-1} \frac{(n-1)!\, S_l^{(n-m)}(0)}{m!\,(n-m-1)!} \sum_{k=0}^{m-1} \frac{(m-1)!}{k!\,(m-k-1)!} T_{l1}^{(m-k)}(0) \left(-S_{l1}^{(k+1)}(0) \right). \tag{22}$$

Here

$$\left(\frac{\partial^n y}{\partial \varphi^n} \right)_{\omega 0} = \frac{\mu_\delta u_\delta h_\delta}{\tau_\omega} \sum_{m=0}^{n-1} \frac{(n-1)!\,(-1)^m}{(n-m-1)!} \left(\frac{\partial^{n-m-1} \tilde{h}}{\partial \varphi^{n-m-1}} \right)_{\omega 0} p^m,$$

$$n = 1, 2, 3, \ldots,$$

$$\left(\frac{\partial^n \tilde{h}}{\partial \varphi^n} \right)_{\omega 0} = \left(\frac{\partial \tilde{h}}{\partial \varphi} \right)_{\omega 0} S_l^{(n)}(0) - \tilde{u}_\delta^2 R_{l0}^{(n)}(0),$$

$$n = 2, 3, \ldots,$$

$$T_l(0) = 1,$$

$$T_l^{(n)}(0) = n \frac{\partial p}{\partial x} \frac{1}{\tau_\omega} \left(\frac{\partial^n y}{\partial \varphi^n} \right)_{\omega 0} - \sum_{m=1}^{n} \frac{n!\, T_l^{(n-m)}(0)\, p^m}{m!\,(n-m)!},$$

$$n = 1, 2, 3, \ldots$$

Formulas (21) and (22) can be applied to the coefficients of the expansion in the turbulent portion of the flow, but everywhere in these we have to replace $S_{l1}^{(n)}(0)$ by $S_{t1}^{(n)}(\varphi_l)$, Pr_l by Pr_t, $T_{l1}^{(n)}(0)$ by $T_{t1}^{(n)}(\varphi_l)$, $R_{l1}^{(n)}(0)$ by $R_{t1}^{n}(\varphi_l)$, and we have to bear in mind that the expressions for the derivatives $\partial^n y/\partial\varphi^n$ and $\partial^n \tilde{h}/\partial\varphi^n$, as well

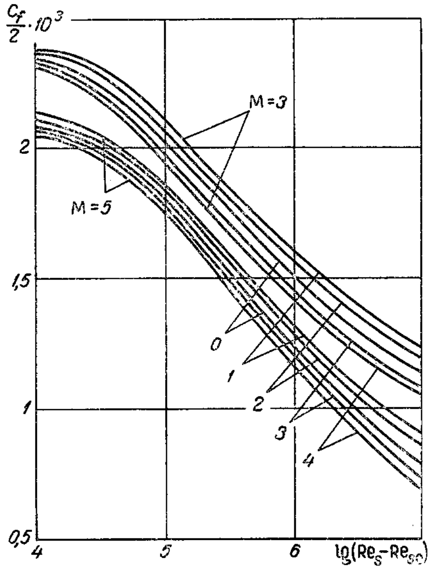

Fig. 3

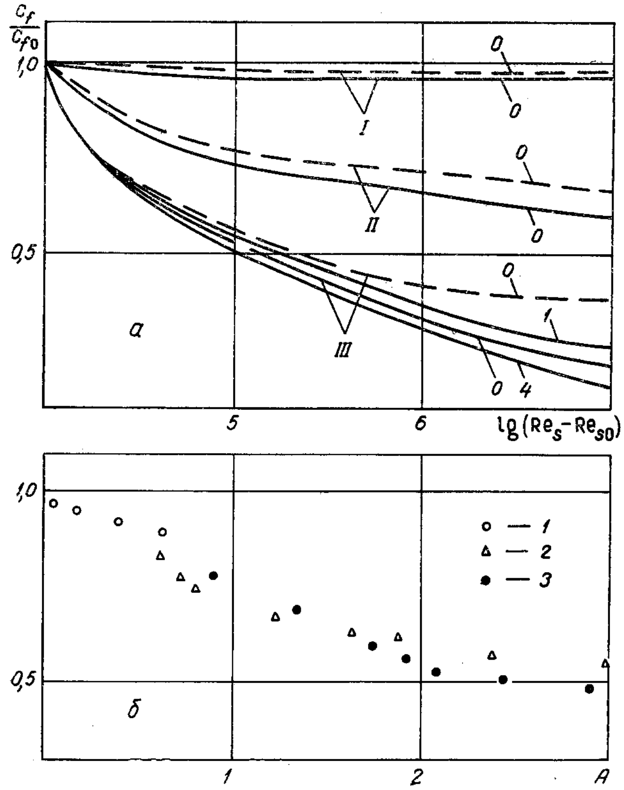

Fig. 4

Fig. 3. Change in the coefficient of surface friction along the flow for various diffuser divergence angles: 1) α = 8°; 2) 4°; and for various convergence angles: 3) α = 4°; 4) 8°; 0 denotes flow along the plate.

Fig. 4. Variation in the ratio c_f/c_{f0} along the flow (a) (numerical notation for the curves is the same as in Fig. 3; the solid curves) for M_{in} = 5; the dashed curves are for a value of 3; I) c = 0.0005; II) 0.005; III) 0.01) and as a function of the injection parameter (b) for various quantities of injected material: 1) c = 0.0005; 2) 0.005; 3) 0.01.

as for $T_{t1}^{(n)}(\varphi_l)$ in the turbulent sublayer are different and are written in the form

$$\left(\frac{\partial y}{\partial \varphi}\right)_l = \frac{k}{\sqrt{\frac{c_f}{2}}} \frac{\delta_l}{\sqrt{\tilde{h}_l \tilde{\tau}_l}},$$

$$\left(\frac{\partial^n y}{\partial \varphi^n}\right)_{l0} = \frac{1}{\sqrt{\tilde{h}_l \tilde{\tau}_l}} \left[\frac{k}{\sqrt{\frac{c_f}{2}}} \frac{\partial^{n-1} y}{\partial \varphi^{n-1}} - (n-1)! \sum_{m=1}^{n-1} \frac{1}{m!\,(n-m-1)!} \right.$$

$$\left. \times \frac{1}{\sqrt{\tilde{h}_l \tilde{\tau}_l}} \frac{\partial^{n-m} y}{\partial \varphi^{n-m}} \left[\frac{\partial^m (\tilde{h}\tilde{\tau})}{2\partial \varphi^m} - (m-1)! \sum_{k=1}^{m-1} \frac{1}{k!\,(m-k-1)!} \frac{\partial^{m-k}(\sqrt{\tilde{h}\tilde{\tau}})}{\partial \varphi^{m-k}} \frac{\partial^m (\sqrt{\tilde{h}\tilde{\tau}})}{\partial \varphi^m} \right] \right]_{l0},$$

$$n = 2, 3, \ldots,$$

$$\left(\frac{\partial^n \tilde{h}}{\partial \varphi^n}\right)_{l0} = \left(\frac{\partial \tilde{h}}{\partial \varphi}\right)_{\omega 0} S_0^{(n)}(\varphi_n) - \tilde{u}_\delta^2 R_0^{(n)}(\varphi_l),$$

$$n = 2, 3, \ldots,$$

$$T_l(\varphi_l) = 1 + \frac{1}{\tau_\omega \tilde{\tau}_l} \frac{\partial p}{\partial x} \varphi_l \left(\frac{\partial y}{\partial \varphi}\right)_{l0},$$

$$T_l^{(n)}(\varphi_l) = \frac{1}{\tilde{\tau}_l} \left[\frac{n}{\tau_\omega} \frac{\partial p}{\partial x} \frac{\partial^n y}{\partial \varphi^n} + \frac{\frac{\partial p}{\partial x}\varphi_l}{\tau_\omega} \frac{\partial^{n+1} y}{\partial \varphi^{n+1}} - \sum_{m=1}^{n} \frac{n!\, T^{(n-m)} \tilde{\tau}^{(m)}}{m!\,(n-m)!} \right]_{l0}.$$

$$n = 1, 2, 3, \ldots$$

TABLE 1. Effect of a Change in the Pressure Gradient for Various Quantities of Inflowing Matter on the Ratios: I) of the Thickness of the Laminar Sublayer to the Thickness of the Boundary Layer (δ_l^*/δ); II) of the Momentum Thickness to the Thickness of the Boundary Layer (δ^{**}/δ); III) of the Displacement Thickness to the Momentum Thickness (δ^*/δ^{**}) (when M = 5, h_ω = 5)

c	φ_l	Re_{in} = 10^7, α = 0°	10^7, 2°	10^7, 8°	10^6, 2°	10^6, 8°	10^5, 2°	10^5, 8°
				I				
0	0,7	0,168	0,170	0,187	0,167	0,168	0,180	0,183
	0,6	0,052	0,053	0,046	0,046	0,048	0,055	0,061
	0,5	0,008	0,010	0,007	0,007	0,009	0,011	0,017
	0,4	0,001	0,004	0,004	0,001	0,001	0,002	0,003
	0,3	0,000	0,000	0,000	0,000	0,000	0,000	0,000
0,001	0,7	0,179	0,179	0,179	0,179	0,183	0,183	0,191
	0,6	0,056	0,057	0,057	0,157	0,063	0,059	0,080
	0,5	0,012	0,012	0,012	0,012	0,012	0,018	0,025
	0,4	0,002	0,001	0,001	0,001	0,001	0,004	0,008
	0,3	0,000	0,000	0,000	0,000	0,000	0,000	0,000
0,005	0,7	0,223	0,223	0,223	0,223	0,224	0,226	0,231
	0,6	0,096	0,097	0,097	0,097	0,099	0,102	0,110
	0,5	0,037	0,036	0,036	0,037	0,037	0,044	0,058
	0,4	0,011	0,011	0,011	0,012	0,014	0,016	0,024
	0,3	0,003	0,003	0,004	0,006	0,005	0,011	0,017
				II				
0	0,7	0,039	0,033	0,034	0,037	0,038	0,038	0,038
	0,6	0,038	0,037	0,037	0,037	0,037	0,037	0,039
	0,5	0,038	0,033	0,033	0,034	0,034	0,036	0,040
	0,4	0,026	0,026	0,026	0,027	0,029	0,030	0,036
	0,3	0,021	0,021	0,022	0,021	0,023	0,024	0,027
0,001	0,7	0,039	0,038	0,039	0,038	0,038	0,038	0,038
	0,6	0,038	0,038	0,038	0,038	0,038	0,038	0,038
	0,5	0,036	0,036	0,036	0,036	0,036	0,037	0,039
	0,4	0,030	0,030	0,030	0,030	0,031	0,035	0,039
	0,3	0,026	0,026	0,027	0,028	0,027	0,032	0,039
0,005	0,7	0,039	0,039	0,039	0,039	0,039	0,039	0,040
	0,6	0,040	0,040	0,040	0,040	0,040	0,041	0,041
	0,5	0,040	0,040	0,040	0,040	0,040	0,041	0,042
	0,4	0,037	0,037	0,037	0,037	0,038	0,039	0,043
	0,3	0,036	0,036	0,037	0,038	0,039	0,040	0,043
				III				
0	0,7	13,02	12,91	13,02	12,96	12,96	12,99	13,14
	0,6	11,52	11,34	11,21	11,22	11,26	11,34	11,66
	0,5	10,70	9,72	9,74	9,89	9,97	9,99	10,89
	0,4	10,22	7,57	7,64	7,84	8,56	9,31	10,53
	0,3	7,54	7,00	7,32	7,52	8,99	9,92	11,00
0,001	0,7	13,09	13,09	13,09	13,09	13,10	13,14	13,27
	0,6	11,40	11,40	11,40	11,41	11,41	11,51	11,82
	0,5	10,09	10,07	10,08	10,10	10,14	10,39	11,06
	0,4	8,66	8,65	8,70	8,79	8,75	9,67	11,03
	0,3	8,52	8,65	8,61	8,80	8,63	10,01	11,21
0,005	0,7	13,60	13,60	13,60	13,60	13,61	13,64	13,75
	0,6	12,02	12,02	12,02	12,02	12,05	12,10	12,35
	0,5	11,00	10,93	10,94	10,95	11,01	11,12	11,64
	0,4	10,11	10,12	10,14	10,16	10,30	10,56	11,67
	0,3	10,01	9,98	10,03	10,06	10,13	10,53	11,42

The heat content is thus given in the form of a function of velocity:

when $y \leq \delta_l$

$$\tilde{h}_1 = \tilde{h}_{\omega 1} + \left(\frac{\partial \tilde{h}}{\partial \varphi}\right)_{\omega 1} S_l(\varphi) - \tilde{u}_\delta^2 R_l(\varphi), \qquad (23)$$

when $y \geq \delta_l$

$$\tilde{h}_1 = \tilde{h}_{\omega 1} + \left(\frac{\partial \tilde{h}}{\partial \varphi}\right)_{\omega 1} S_1(\varphi) - \tilde{u}_\delta^2 R_1(\varphi), \qquad (24)$$

where

$$S_1(\varphi) = S_l(\varphi_l) + \frac{1}{\mathrm{Pr}_l} S'_l(\varphi_l) S_t(\varphi),$$

$$R_1(\varphi) = R_l(\varphi_l) + R'_l(\varphi_l) S_{t1}(\varphi) + R_t(\varphi).$$

Integrating (7) and (9) in conjunction with (5), (6), (14), (23), and (24), in first approximation we obtain the following velocity profiles:

when $y \leq \delta_l$

$$y_1 = \frac{\mu_\delta}{\rho_\delta u_\delta \frac{c_f}{2}} \left[\frac{\tilde{h}_\omega \ln \tilde{\tau}_l}{P} + \sum_{n=0}^{\infty} \left\{ \frac{1}{n!} \left[\left(\frac{\partial \tilde{h}}{\partial \varphi} \right)_{\omega 1} S_l^{(n)}(\varphi) - \tilde{u}_\delta^2 R_l(\varphi) \right] \sum_{k=0}^{n-1} \left[\frac{(-1)^k \varphi^{n-k}}{(n-k) P^{k+1}} + \frac{(-1)^n \ln \tilde{\tau}}{P^{n+1}} \right] \right\} \right],$$

when $y \geq \delta_l$

$$y = \delta_l \exp\left[\frac{k}{\sqrt{\frac{c_f}{2}}} \int_{\varphi_l}^{\varphi} \frac{d\varphi}{\sqrt{(1 + P\varphi)\tilde{h}_1}} \right].$$

The subsequent approach to the solution in the first approximation is the same as in the zeroth approximation and the problem, as before, reduces to the numerical solution of (18).

As an example we calculated the flows in flat converging and diverging sections of a diffuser with various angles of divergence ($\alpha \sim 2°$-$8°$) at a constant wall temperature ($\tilde{h}_\omega$ = const). The coordinate x was reckoned along the wall from the point of intersection for the extension of the walls, and y was reckoned in a direction normal to x within the channel. The boundary layer was assumed to be turbulent from some initial cross section with the coordinate x_0, and the following quantities were specified within that section: Re_{in} ($\sim 10^5$-10^7), M_{in}(3-5), and Re_{in}^{**} (~ 300). At the edge of the boundary layer all of the flow parameters were assumed to be known from the condition of the one-dimensional isentropic flow of an ideal compressible fluid. For such a flow, the following relationships have been established [4] between the parameters in the various cross sections:

$$\frac{M}{M_{in}} = \frac{x_{in}}{x} \left[\frac{1 + \frac{\gamma - 1}{2} M^2}{1 + \frac{\gamma - 1}{2} M_{in}^2} \right]^{\frac{\gamma+1}{2(\gamma-1)}}, \quad \frac{T}{T_{in}} = \frac{1 + \frac{\gamma - 1}{2} M_{in}^2}{1 + \frac{\gamma - 1}{2} M^2}, \quad \frac{p}{p_{in}} = \left[\frac{1 + \frac{\gamma - 1}{2} M_{in}^2}{1 + \frac{\gamma - 1}{2} M^2} \right]^{\frac{\gamma}{\gamma-1}}.$$

In the calculations it is assumed that Pr_l = 0.7 and Pr_t = 1.0. The injection of the material is specified on the basis of the law v_ω / v_{in} = c.

We give the result from the calculation of the zeroth approximation. Initially without solution for the equation of the momenta, let us establish the relationships between certain of the parameters of the turbulent boundary layer and the velocity at the edge of the laminar sublayer, which are obtained from the numerical solution of (15) and (17).

Figure 1 shows the change in the coefficient of surface friction with a change in φ_l for flows with various pressure gradients ($\alpha \sim 2°$-$8°$), and with various injections of matter (b $\sim 10^{-4}$-10^{-2}) for various ranges in Re_{in}(10^5-10^7) and in M_{in}(0.8, 3.0, 5.0). For comparison, here we find the curve for $c_f/2 = \varphi_l^2/(k_1/k)^2$, i.e., the relationship between $c_f/2$ and φ_l for a plate in an incompressible fluid, in the absence of injection. We see from Fig. 1 that these curves differ from each other only in the value of M_{in} and in $\tilde{h}_\omega$. For these M_{in} and $\tilde{h}_\omega$ the points applicable to flows with various pressure gradients and different values of Re_{in} and b virtually group about a single curve, which coincides with the curve for a plate in the absence of injection. This permits us to draw the conclusion that for various flows (with pressure gradients) in which there is an inflow of material we can retain the same form for the relationship between $c_f/2$ and φ_l as in the case of a flow without a pressure gradient and without injection of fresh material (i.e., we assume

P = 0), and namely

$$\sqrt{\frac{c_f}{2}} = \frac{\varphi_l}{(k_1/k)} \frac{\left[\tilde{h}_\omega + \left(\frac{\partial \tilde{h}}{\partial \varphi}\right)_\omega \frac{\varphi_l}{2} - \Pr_l \frac{\tilde{u}_\delta^2}{6} \varphi_l^2\right]}{\tilde{h}_l^{3/2}},$$

and here

$$\tilde{h}_l = \tilde{h}_\omega + \left(\frac{\partial \tilde{h}}{\partial \varphi}\right)_\omega \varphi_l - \frac{\tilde{u}_\delta^2}{2} \Pr_k \varphi_l^2.$$

For a cold wall the coefficient of surface friction is larger. The curves showing $c_f/2$ as a function of φ_l for $\tilde{h}_\omega = 1.0$ (the dashed curves) shift upward in comparison with the curve for $\tilde{h}_\omega = 5$ (solid lines). The presence of a pressure gradient and the injection of material, all other conditions being equal, have little effect on the relationship between the heat content at the edge of the laminar sublayer and φ_l. Figure 2a shows the change in $\tilde{h}_l$ as a function of φ_l for various values of M_{in} and b. The points which relate to flows with various pressure gradients and with injection (b and Re_{in}) for given M_{in} and $\tilde{h}_\omega$ virtually group about a single curve. It is therefore possible, with sufficient accuracy, to use the same form of the relationship between the content and velocity in flows with injection and a pressure gradient (in the laminar sublayer, in any case) as in the streamlining of a plate in the absence of injection, and namely (see [2], p. 288):

when $y \le \delta_l$

$$\tilde{h} = \tilde{h}_\omega + \left(\frac{\partial \tilde{h}}{\partial \varphi}\right)_\omega \varphi_l - \Pr_л \tilde{u}_\delta^2 \frac{\varphi_l^2}{2},$$

when $y \ge \delta_l$

$$\tilde{h} = \tilde{h}_\omega + \left(\frac{d\tilde{h}}{d\varphi}\right)_\omega \left[\frac{\varphi}{\Pr_l} - \left(1 - \frac{1}{\Pr_l}\right)\varphi_l\right] - \tilde{u}_\delta^2 \left[\frac{\varphi^2}{2} - (1 - \Pr_l)\frac{\varphi_l^2}{2}\right].$$

From Fig. 2a we see that the heat flow from the hot wall increases with a reduction in M_{in} and that there is a reduction in the heat flow to the cold wall. Figure 2b shows the effect of the injection of matter on the change in the St number as a function of φ_l for various M_{in}. The injection of matter at the constant M number in the inlet section increases the heat flow from the hot wall and reduces the heat flow to the cold wall; the St number as a function of φ_l changes only slightly in this case.

To determine the effect of the pressure gradient in the relationship between the thermal characteristics and φ_l, we calculated the first approximation. Consideration of the five terms in (19) and (20) ensured all of the required accuracy for the solution. It turned out that the results of the zeroth and first approximations for semidiverging channel angles from 2° to 8° are correct to 0.5-1.0% over the entire range of variation in φ_l.

With regard to the effect of the pressure gradient on the nature of the variation as a function of φ_l for such ratios as δ_l/δ, δ^{**}/δ, and δ^*/δ^{**}, we can say exactly what was said with regard to the above-cited quantities, and namely, all other conditions being equal, the pressure gradient has virtually no effect on the variation of these ratios as a function of velocity at the boundary of the laminar sublayer.

This is illustrated by Table 1 showing the ratios δ_l/δ, δ^{**}/δ, and δ^*/δ^{**}, respectively, for various pressure gradients and injections. Thus, proceeding from the above, we can assume that consideration of the pressure gradient in the equation of momenta alone will be as accurate in terms of the solution as the method described above.

Let us turn to the results of the numerical solution of the equation of momenta (18). Figure 3 shows the variation in the coefficient of surface friction along the flow in the absence of injection. The comparison is performed for identical differences in the Re numbers for the section under consideration and the initial section. With negative pressure gradients, the coefficient of surface friction increases in comparison with the case of flow on a plate. For positive pressure gradients the situation is the opposite. We note that in a supersonic flow the existence of a pressure gradient has less effect on the variation in the coefficient of surface friction than in the case of an incompressible fluid. The introduction of material reduces the effect of the pressure gradient even further. The entire family of cited curves (for the given M_{in}) in the case of large injections (c = 0.01) virtually merges into a single curve.

Figure 4a shows the change in c_f/c_{f_0} along the flow for various values of c. The curves for flows with pressure gradients are given only for strong injection (c = 0.01) and M_{in} = 5.0, so as not to burden the figure. For other quantities of injected material and for M_{in} = 3 the shape of the curves is the same. With a reduction in the M_{in} number, the effectiveness of the injection is diminished. For compressible fluids the coordinates $\zeta = (c_f/2)(Re^{**})^{1/4}$ (the parameter of the friction law), $\Gamma = (\delta^{**}/u_\delta)(du_\delta/dx)(Re^{**})^{1/4}$ (the parameter of the pressure gradient), and A (the injection parameter), as in the case of incompressible fluids, are not entirely suitable for the plotting of universal curves. Figure 4b shows the change in the ratio c_f/c_{f_0} on a plate (Γ = 0) as a function of A. We see that although the plotted points are grouped rather tightly, they do not fall on a single curve. The greater the magnitude of the influx material, the more pronounced in the reduction in c_f/c_{f_0} with an increase in A.

NOTATION

x, y	are, respectively, the longitudinal and transverse coordinates;
v_x, v_y	are, respectively, the longitudinal and transverse components of velocity;
ρ	is the density;
μ	is the viscosity;
τ	is the sheer stress;
h	is the heat content;
q	is the heat flow;
u	is the free-stream velocity;
δ	is the thickness of the boundary layer;
δ^*	is the displacement thickness;
δ^{**}	is the momentum thickness;
c	is the coefficient of surface friction (c_{f_0} is the surface friction in the absence of injection);
v_ω	is the velocity of injection;
k = 0.39, k_1 = 4.3	are empirical turbulence constants;
α	is the half-angle of channel divergence;
S	is the longitudinal coordinate reckoned along the flow from the point of boundary-layer formation (S_0 is the coordinate of the cross section from which the boundary layer is assumed to be turbulent);
$\varphi = v_x/u_\delta$;	
$\tilde{h} = h/h_\delta$;	
$\tilde{u}_\delta = u/\sqrt{h_\delta}$;	
$Re^{**} = (\rho_\delta u_\delta/\mu_\delta)\delta^{**}$;	
$Re_S = (\rho_\delta u_\delta/\mu_\delta)S$	are Reynolds numbers;
St	is the Stanton number
M	is the Mach number

Subscripts

δ	denotes conditions at the edge of the boundary layer;
l	denotes conditions at the edge of the laminar sublayer;
ω	denotes conditions at the wall;
in	denotes conditions in the inlet cross section.

LITERATURE CITED

1. I. P. Ginzburg and N. S. Krest'yaninova, "Gasdynamics and heat transfer," Sb. 1, Uch. Zap. LGU, No. 338, Ser. Matem. Nauk, No. 43, 50 (1968).
2. I. P. Ginzburg, Aerogasdynamics [in Russian], Vysshaya Shkola, Moscow (1966).
3. I. P. Ginzburg, "Gasdynamics and heat transfer," Sb. 1. Uch. Zap. LGU, No. 338, Ser. Matem. Nauk. No 43, 36 (1968).
4. L. A. Vulis, The Thermodynamics of Gas Flows [in Russian], Gosenergoizdat (1950).